LA-UR- 04-2594

Approved for public release;
distribution is unlimited.

Title: Detailed Characterization of Plasma Wave Behavior Using Collective Thomson Scattering

Author(s): David S. Montgomery, P-24
John L. Kline, P-24
Thomas E. Tierney, P-24

Submitted to: proceedings for:
High Temperature Plasma Diagnostics Conference
April 19 - 22, 2004
San Diego, CA
to be published in Review of Scientific Instruments

LOS ALAMOS NATIONAL LABORATORY
3 9338 00435 7256

Los Alamos
NATIONAL LABORATORY

Los Alamos National Laboratory, an affirmative action/equal opportunity employer, is operated by the University of California for the U.S. Department of Energy under contract W-7405-ENG-36. By acceptance of this article, the publisher recognizes that the U.S. Government retains a nonexclusive, royalty-free license to publish or reproduce the published form of this contribution, or to allow others to do so, for U.S. Government purposes. Los Alamos National Laboratory requests that the publisher identify this article as work performed under the auspices of the U.S. Department of Energy. Los Alamos National Laboratory strongly supports academic freedom and a researcher's right to publish; as an institution, however, the Laboratory does not endorse the viewpoint of a publication or guarantee its technical correctness.

Form 836 (8/00)

Detailed Characterization of Plasma Wave Behavior Using Collective Thomson Scattering

D.S. Montgomery, J.L. Kline, T.E. Tierney IV

Plasma Physics Group, Physics Division, Los Alamos National Laboratory

Los Alamos, NM 87545

Collective Thomson scattering is widely used to measure bulk plasma parameters in high density, laser-produced plasmas, and is used to detect plasma waves from instabilities. However, inhomogeneity in these small plasmas often leads to a spectrum with insufficient resolution to discern phenomena such as wave damping and nonlinear wave effects. Two techniques are discussed for laser-produced plasmas to overcome these limitations, and provide details of wave damping and nonlinear behavior. First, imaging Thomson scattering is used to obtain spatially-resolved plasma wave profiles in a 100 – 200 eV plasma, and allows us to infer ion-ion collisional damping rates. Second, a diffraction-limited laser beam is used to drive stimulated Raman scattering (SRS) in a hot plasma, generating large amplitude Langmuir waves. The comparatively small interaction volume permits sufficient spectral resolution to observe nonlinear wave behavior, previously unresolved in other experiments.

PACS numbers: 52.38.Bv, 52.70.Kz, 52.35.Fp, 52.35.Mw

I. Introduction

Plasma waves are a significant topic in plasma physics, and govern many important phenomena including energy transport, turbulence, and propagation of electromagnetic waves within the plasma. Such collective modes occur naturally in plasmas, and may exist as small amplitude fluctuations near thermal equilibrium, or can be driven to very large amplitudes by sources of free energy. In the limit of thermal-level fluctuations, the frequency, wavelength, and damping are defining characteristics of the wave behavior. For very large amplitude waves, nonlinear effects such as instabilities, coupling to other plasma waves, and particle trapping, also become important.

Collective Thomson scattering from a laser probe is often used to diagnose waves in plasmas, and can be used to measure bulk plasma characteristics such as electron density (n_e), electron and ion temperature (T_e, T_i), as well as plasma flow (u). In principle, Thomson scattering can be used to measure wave damping rates and nonlinear effects. In a laser-produced plasma, such as those used in laser-fusion research, the plasma scale lengths are quite small (100's μm), and plasma non-uniformity within the probe volume often masks the ability to measure wave damping and nonlinear wave effects.

In this paper, we report two techniques developed to overcome these limitations in laser-produced plasmas. For experiments designed to measure wave damping, we employ imaging Thomson scattering to obtain spatially-resolved snapshots of the scattered light spectra from thermal-level waves. Profiles of the density, temperature, and flow are measured from the spatially-resolved spectra, which allow us to fully account for broadening effects due to plasma inhomogeneity, and obtain a measure of wave damping.

To measure nonlinear wave effects due to laser-plasma instabilities from an intense laser beam, a nearly diffraction-limited laser (single hot spot) is used to drive instabilities in a preformed plasma. Thomson scattering from a second, lower intensity beam is used to detect the driven plasma waves associated with these instabilities. The interaction volume in these experiments is much smaller than the plasma gradient scale lengths so that the interaction occurs in extremely uniform conditions, which allows detection of the subtle signatures often associated with many nonlinear wave phenomena.

This paper is organized as follows: the background material for detecting wave behavior in nonuniform plasmas is given, and an overview of Thomson scattering is presented in Sec. II. Sec. III describes the technique used to measure plasma wave damping in the presence of plasma nonuniformity. In Sec. IV, we discuss the experimental and diagnostic technique used to measure nonlinear effects due to large amplitude waves driven by laser-plasma instabilities in a nonuniform plasma. A summary and concluding remarks are given in Sec. V.

II. Background and Motivation

Since their invention in 1960, the power of lasers has increased remarkably throughout the past four decades. Very high laser power is required (typically 10's to 100's TW) to achieve the conditions necessary for applications such as laser-fusion and high energy-density plasma physics, but can only be achieved for time-scales of order several nanoseconds due to energy limitations.

The laser energy limits the achievable plasma size for these applications, making detailed diagnosis a challenge. The plasma size scales as $s \approx \left(\varepsilon E_L / n_e k_B T_e\right)^{1/3}$, where E_L is the laser energy, n_e and T_e are the plasma electron density and temperature, k_B is

Boltzmann's constant, and ε represents the effective coupling efficiency of laser energy into electron thermal energy. Consider an example where one wants to create a laser produced plasma with $n_e = 10^{21}$ cm^{-3}, $T_e = 3$ keV. Assuming a typical coupling efficiency $\varepsilon = 0.1$, lasers with energy E_L of 1 kJ, 30 kJ, and 1000 kJ will produce plasmas of size 600 μm, 1800 μm, and 6000 μm respectively. By standards in the rest of the plasma community, these laser-produced plasmas are incredibly small.

Plasma inhomogeneity has nearly been a bane for progress in laser-produced plasma experiments due to small plasma sizes. Persistence in diagnostic development has yielded significant advances in spatial and temporal resolution, with values $\delta x \sim 10$ μm and $\delta t \sim 30$ psec being typical. However, plasma gradient scale lengths are nominally of the order $L_n \sim 100$'s μm. For 1-D self-similar expansion into vacuum[1], the approximate density and velocity profiles expanding along an axis z scale as

$$\begin{aligned} n_e(z) &\approx n_0 \exp[-z/L_n] \\ u(z) &\approx c_s + z/\tau \end{aligned} \qquad (1)$$

where n_0 is some initial density, c_s is the ion sound speed, τ is the laser pulse length, and the density gradient scale length $L_n \approx c_s\tau$. As an example, consider a 1 keV carbon plasma so that $c_s \sim 2 \times 10^7$ cm/sec, and for a pulse length $\tau = 1$ nsec, the density scale length is $L_n \approx 200$ μm. Sampling over a 10 μm spatial region near a density $n_0 \sim 10^{21}$ cm^{-3} would result in a density nonuniformity $\Delta n/n \sim 5\%$, and a velocity nonuniformity $\Delta M = \Delta u/c_s \sim 5\%$. This level of uniformity is insufficient to resolve the subtle features in Thomson scattered spectra associated with wave damping and nonlinear effects, as will be discussed next.

Laser-based Thomson scattering produces a frequency-shifted scattered light spectrum due to the motion of free electrons in the laser electric field[2]. A laser with angular frequency and wave-number (ω_0, k_0), incident on a plasma ($\omega_0^2 >> \omega_p^2 = 4\pi n_e e^2/m_e$, the plasma frequency), will produce scattered light (ω_s, k_s) that is shifted in frequency and wave-number due to scattering from electron density fluctuations of frequency and wave-number (ω, k). The scattering process conserves energy and momentum so that frequency and wave-vector matching conditions must be met, $\omega_0 = \omega + \omega_s$, $\vec{k}_0 = \vec{k} + \vec{k}_s$, and is depicted in Fig. 1. The scattering geometry is usually chosen to probe electron density fluctuations with wavenumber $|k| = \sqrt{k_0^2 + k_s^2 - 2k_0 k_s \cos\theta}$, where θ is the angle between the incident laser and the observation direction. Collective (coherent) Thomson scattering is used to observe plasma waves. In this regime, the scattering geometry is chosen such that the wavelength of the density fluctuation is much larger than the electron Debye length ($k\lambda_D << 1$). Thus, scattering occurs from correlated long-wavelength density fluctuations (waves) rather than from the random motions of individual electrons since the electric field of an individual electron is screened for distances greater than the Debye length $\lambda_D = v_e/\omega_p$, where v_e is the electron thermal speed. The Thomson scattered spectrum in the collective regime has resonant peaks at frequencies $\omega_s = \omega_0 \pm \omega$ corresponding to plasma waves with frequency and wavenumber (ω, k). In the absence of plasma inhomogeneity, the width of the scattered light spectrum associated with thermal-level waves is proportional to the wave damping, i.e. weak damping corresponds to narrow peaks, and strong damping corresponds to broadened peaks.

In unmagnetized plasmas, the plasma supports two natural electrostatic modes, namely high-frequency electron plasma waves (EPW or Langmuir waves), and low-frequency ion acoustic waves (IAW), in addition to light waves. The approximate dispersion relations for these waves are $\omega_{epw}/\omega_p \approx 1 + 3/2(k_{epw}\lambda_D)^2$, and $\omega_{iaw} \approx c_s k_{iaw} + \vec{k}_{iaw} \cdot \vec{u}$. Thus, the EPW frequency depends locally on the values of n_e, and T_e, and the IAW frequency depends locally on the values of T_e, and u, so that plasma inhomogeneity can broaden the observed resonances. We next consider examples illustrative of the level of homogeneity required to measure detailed wave behavior.

Stimulated Raman scattering (SRS) is an instability whereby an intense laser wave resonantly decays into a scattered light wave and an EPW, and is important to laser fusion[1]. The growth of the unstable SRS process is typically saturated by EPW nonlinear effects. One nonlinear effect that is important in some regimes is Langmuir decay instability (LDI) cascade, where the EPW generated by SRS can spawn a cascade of multiple EPWs and IAWs. The wave-number and frequency separation (Δk, $\Delta\omega$) between two co-propagating EPW involved in LDI cascade[3] is $\Delta k\lambda_D \approx (4/3)(c_s/v_e)$, and $\Delta\omega/\omega_p \approx 3k\lambda_D(\Delta k\lambda_D)$, where $\Delta\omega/\omega_p \sim 0.015$ for typical conditions. In the presence of a density nonuniformity, LDI cascade will not be resolved if $\Delta n/n > 1.5\%$ within the probed volume of driven waves. Another important nonlinear mechanism is electron trapping, where the EPW has a nonlinear frequency shift $\Delta\omega$ which is proportional to the amplitude of the wave, and increases with $k\lambda_D$, with $(\Delta\omega/\omega_p) \sim -0.01$ given as a typical value for the nonlinear frequency shift.

As an example of the requirements needed to measure wave damping, for an ion-wave damping rate $\nu/\omega_{iaw} \sim 0.1$ the spectral peak will be broadened by approximately

this amount due to the damping alone. If the probed volume contains a velocity gradient, the spectrum will also be Doppler broadened by $\Delta\omega/\omega_{iaw} \approx \Delta u/c_s = \Delta M$. To measure the damping with 10% accuracy requires $\Delta M < 5\%$. The above examples show the stringent homogeneity requirements needed to discern the subtle spectral features associated with these phenomena. In the next sections, we describe techniques used to overcome these limitations for Thomson scattering in laser-produced plasmas.

III. Measuring Ion-Collisional Damping in Inhomogeneous Laser Plasmas

Ion collisional damping becomes important in plasmas with high ionization state Z, high density and low temperatures. Such conditions can occur in the highly ionized Au wall of laser-fusion hohlraum targets, and may be found in other high-energy density plasma regimes. A measure of ion collisionality is the ratio of the ion-ion mean-free-path to the IAW wavelength, or more conveniently $k_{iaw}\lambda_{ii}$, where $k_{iaw}\lambda_{ii} >> 1$ indicates the collisionless regime[4]. We are interested in measuring collisional damping rates in moderately ion-collisional plasmas $(0.1 < k_{iaw}\lambda_{ii} < 10.0)$ where some discrepancies exist between various theoretical models[4]. The laser-plasma conditions needed to operate in this regime dictate a fairly small plasma size (a few hundred microns) due to significant absorption of the laser probe beam and scattered light if the plasma size were much larger[4]. Numerical simulations and previous experiments show that the electron temperature is fairly isothermal in space. Since the IAW dispersion goes as $\omega_{iaw} \approx c_s k_{iaw} + \vec{u} \cdot \vec{k}_{iaw}$, Doppler broadening of the IAW due to velocity gradients in the probe volume is the dominant broadening mechanism for Thomson scattered light in these experiments.

The experiments are performed at the Los Alamos Trident Laser Facility[5] using a Joule-level 527-nm beam to heat a thick CH or Al foil in a 1-ns pulse. The laser focal spot size is ~ 250 μm in diameter and is spatially smoothed using a Random Phase Plate (RPP)[6]. A 351-nm laser is used to probe the plasma at a distance ~ 200 μm from the target surface a few hundred psec after the plasma has formed, and the probe duration is ~ 200 psec. The diagnostic setup for this experiment is shown in Fig. 2. The 351-nm probe is focused using an f/13 lens, and the Thomson scattered light is collected using an f/4 achromatic lens. The central angle defining the scattering geometry is 135°, and the range of angles due to the probe and collection optics produce a wave-number spread $\Delta k/k_{iaw}$ ~ 0.065.

The scattered light from the probed volume is relayed to two separate spectroscopy stations. For the IAW measurements, the Thomson scattered light is imaged onto the entrance slit of a 0.5-m Chromex imaging spectrometer. The image is oriented such that the spectrometer slit images the scattered light along the direction of the probe beam, which corresponds to a radial profile through the plasma. The spectrometer uses a 3600 line/mm holographic grating to obtain 0.4 Å spectral resolution. The width of the spectrometer slit is ~50 μm and, using a 5x magnification in the relay optics, corresponds to a ~ 10 μm sample of the plasma in the direction of the blow off. The spatial resolution in the imaging direction is ~ 10 μm. The spectrum is detected using a Kentech gated optical imager with a ~200 psec framing time, and is read out using a 1024 x 1024 CCD camera. The resulting resolution for the Thomson scatter IAW measurements are $\Delta\lambda$ = 0.4 Å, Δx = 10 μm, and Δt ~ 200 psec. The Thomson scattered spectrum from EPW is

also measured using a similar instrument, and results in a resolution $\Delta\lambda = 3$ nm, $\Delta x = 10$ μm, and $\Delta t \sim 200$ psec.

To avoid further spectral blurring, an additional requirement is that the temporally and spatially dependent changes in the scattered light spectra occur slowly enough such that they are adequately sampled by the resolution of the instruments, i.e. $\frac{\partial\lambda}{\partial x} << \frac{\Delta\lambda}{\Delta x}$, $\frac{\partial\lambda}{\partial t} << \frac{\Delta\lambda}{\Delta t}$, which is simply a restatement of the sampling theorem. This criterion is checked as part of the analysis for the spatially-resolved spectra. To ensure that the scattered light spectra from IAW are not changing on a time-scale faster than the framing time (~200 psec), streaked spectra from IAW were also obtained on these experiments. The separation between the up-shifted and down-shifted IAW peaks was nearly constant over the 200 psec probe duration, indicating a steady temperature and that $\frac{\partial\lambda}{\partial t} << \frac{\Delta\lambda}{\Delta t}$ was satisfied.

A spatially resolved Thomson scattered spectrum from IAW is shown in Fig. 3 for an Al plasma with $n_e \sim 1.2 \times 10^{20}$ cm^{-3}, $T_e \sim T_i \sim 105$ eV, and $k_{iaw}\lambda_{ii} \sim 0.5 - 2.0$. The spectra show a peak-to-peak separation of ~ 3.5 Å, indicative of a fairly isothermal temperature distribution in the radial direction. The spectra show an "S" shape due to Doppler shifts by radially symmetric outward flow, and this shape is expected due to rarefaction. However, since the probe beam is somewhat large compared to the velocity gradient scale lengths, Doppler broadening of each peak also occurs. The spectrum is fit to obtain spatial profiles[4] of T_e and radial flow u. The electron-ion equilibration time is expected to be fairly short, and justifies our assumption that $T_i \sim T_e$. The EPW spectrum

is simultaneously measured, and the spectrum is fit to obtain estimates of the density profile.

As mentioned previously, the dominant inhomogeneity broadening for the IAW spectrum is from velocity gradients in the probe volume, although density and temperature gradients do play a small role in these experiments. Accurate accounting of inhomogeneity broadening and instrumental broadening is critical since we are interested in measuring collisional IAW damping rates. The Thomson scattered spectra are modeled[4] using analytic fits of the velocity vector field $\vec{u}(\vec{r})$, the density $n_e(r)$, and the temperatures $T_e(r)$, $T_i(r)$, where radial symmetry is assumed. These plasma profiles are assigned to a 2-D grid, as shown in Fig. 4. Both a collisionless and a collisional Thomson scattering form factor S(k, ω) is computed at each grid point for the local plasma conditions[4]. The finite range of IAW wave-numbers sampled due to the angular acceptance of the optics ($\Delta k/k_{iaw} \sim 0.06$) is also accounted for by assuming that range of wave-numbers for each grid point, although this is a small effect compared to Doppler broadening. The size of the probe laser beam is accounted for in the plasma, and ultimately dictates the degree to which plasma inhomogeneity broadens the spectra in this experiment[4]. The computed scattered light is then summed for each grid point (within the scattering volume) in the direction of the detector. Inverse bremmstrahlung absorption is taken into account for both the incident probe beam and the scattered light. The synthesized spatially-resolved spectrum is computed, and the spatial and spectral resolution functions are convolved to produce the final synthetic image, as shown in Fig. 5.

To first order, the ion collisional damping rate is proportional to the width of an individual IAW peak. Plotted in Fig. 6 is the width $\delta\omega/\omega_{iaw}$ of the red-shifted IAW peak versus radial position for the experimental data shown in Fig 3. The observed spectral broadening is $\delta\omega/\omega_{iaw} \sim 1.2$. Of this, instrumental effects can account for $\delta\omega/\omega_{iaw} \sim 0.2$, and contributions from inhomogeneity and collisionless damping $\delta\omega/\omega_{iaw} \sim 0.5$. Plotted are the theoretical curves for the broadening assuming either a collisionless or collisional scattering form factor $S(k, \omega)$. The collisional model matches the observed broadening when the plasma inhomogeneity is taken into account, and can provide a measure of ion collisional damping rates in these plasmas[4].

IV. Measuring Nonlinear Effects in Inhomogeneous Laser Plasmas

Parametric instabilities such as stimulated Raman scatter (SRS) occur when an intense laser beam propagates in a laser-fusion plasma[1], and in cases where the instability is far above threshold, plasma wave nonlinear effects typically saturate the growth of SRS. Thus, understanding the nonlinear wave mechanisms can be a key element to predicting the behavior of the instability. As mentioned in Sec. II, two important nonlinear effects for EPW are LDI cascade and electron trapping, both of which require the ability to observe subtle spectral shifts $\Delta\omega/\omega_p \sim 0.01$ in order to discern the underlying behavior. These two competing nonlinear effects are expected be dominant in different regimes[7] of $k\lambda_D$.

Most modern laser-plasma experiments are performed with some type of spatial smoothing, such as random phase plates [RPP], in order to smooth large-scale intensity modulations characteristic of high-power lasers[6]. The smoothing results in an ensemble of much smaller scale hot spots, or speckles, near the focus of the laser, and their

properties can be described statistically. Strong nonlinear effects are expected in the most intense hot spots where the instabilities are driven strongly. As pointed out in Sec. II, probing over even a relatively small volume, defined by a typical instrument spatial resolution of ~ 10 μm, will still result in a density nonuniformity of $\Delta n/n \sim 5\%$ for $L_n \sim$ 200 μm. Thus, the Thomson spectra will be blurred in experiments with RPP-smoothed laser beams, and not allow the detection of subtle spectral features[3]. Indeed, even if it were possible to produce an initially uniform plasma, the ponderomotive pressure of the laser hot spots alone will produce local density nonuniformities $\Delta n/n \sim$ several percent for typical laser-plasma conditions.

To overcome these limitations, we have developed an experimental test-bed using a nearly diffraction-limited laser beam (single hot spot) to interact with a preformed plasma and drive SRS[6, 8]. In many respects, the single hot spot interaction volume mimics one of the speckles of a RPP-smoothed laser beam, where the width of the speckle is $\sim f\lambda$, and the speckle length $\sim 7 f^2 \lambda$, where f is the focal length to diameter ratio of the focusing lens. For our experiment, an interaction beam with $\lambda = 527$-nm is focused to a nearly diffraction limited spot with an *f/4.5* lens so that the speckle width and length are ~2.5 μm and ~ 75 μm respectively. We ensure that the plasma density gradient scale length $L_n >>$ speckle length. However, SRS convective growth means that the effective interaction length is ~ few μm, which is very small compared to L_n, thus the large amplitude waves occur in extremely homogeneous conditions.

These experiments are also performed at the Trident Laser[5] using ~ 400 J in two 527-nm beams to heat a thick CH foil and preform a plasma after the 1 nsec heater pulse. Each heater beam focal spot is ~ 600 μm in diameter and is smoothed with a RPP. The

527-nm single hot spot beam is focused with an *f/4.5* lens parallel to the target surface, and is offset by several hundred μm to systematically vary the plasma density. A low intensity (~ 0.5 J, 200 psec.) 351-nm laser is focused to ~ 150 μm spot to ensure overlap with the single hot spot interaction volume, and arrives simultaneous with the single hot spot beam. The central scattering angle between the probe beam and collection optic is ~ 71°, with ± 18.5° range defined by the *f/4* probe lens and *f/2.5* collection optic. This angular range allows us to explore EPW over a range of $k\lambda_D$ expected for observation of both LDI cascade and trapping effects. The experimental layout is shown in Fig. 7.

Thomson scattered light from EPW in the probed volume is collected and split in two different paths, and relayed to two separate spectroscopy stations. One station contains a streaked spectrometer which integrates over the range of $k\lambda_D$ probed, with spectral and temporal resolution of $\Delta\lambda \sim 1$ Å and $\Delta t \sim 30$ psec. An object lens is used to image the plasma within the probe volume to the entrance slit of an imaging spectrometer, similar to that described in Sec. III. The spectrometer slit and perpendicular streak camera slits define the probe volume, which is much larger than the effective interaction volume (~ few μm^3). A second spectroscopy station provides an angle-resolved spectrum of the Thomson scattered light from EPW by imaging the collection lens plane onto the slit of an imaging spectrometer. The detector provides a ~ 200 psec frame of the angle-resolved spectra, and the data can be directly correlated to (ω, k) of the driven EPWs[9].

One challenge in this experiment is that the EPWs must be driven to fairly large levels to be detected above thermal scattering levels due to the fact that the probe volume is much larger than the interaction volume[8], $V_{probe} >> V_{int}$. The probe beam spot size is

typically ~ 150 μm, so that $V_{probe} \sim (150\ \mu m)^3$, compared to $V_{int} \sim$ few μm^3. As a result, only a very small fraction of the probe beam actually scatters from driven waves, as depicted in Fig. 8. In the case of SRS, the driven EPW are ~ $10^4 - 10^5$ larger than thermal level fluctuations for SRS reflectivity exceeding 1%. The Thomson scattered power scales as $P_{scat} \sim (\Phi_{driven})^2 V_{int} >> (\Phi_{thermal})^2 V_{probe}$, where Φ is the EPW amplitude. Although the probe volume is much larger than the interaction volume, scattering from driven waves completely dominant the observed scattering since $(\Phi_{driven}/\Phi_{thermal})^2 >> V_{probe}/V_{int}$. A caveat of the single hot spot technique is that one cannot directly measure Φ_{driven} from the Thomson scattered power unless V_{int} is independently measured, which is difficult for a volume ~ few μm^3. In contrast, RPP experiments typically produce driven waves throughout the probe volume so that at least an RMS (space and time-averaged) wave amplitude can usually be directly determined from the Thomson scattered power. Fortunately, the driven wave amplitudes may be estimated by other means in the single hot spot experiment so that meaningful information about the waves can still be obtained.

Figures 9a – 9c show streaked spectra of Thomson scattering from EPW in a single hot spot experiment. The density is systematically varied by a small factor in Fig. 9a - 9c to vary $k\lambda_D$, and T_e decreases slightly on each shot so that there is also a small decrease in $k\lambda_D$ with time for each streak. In Fig. 9a, multiple EPW are observed and the scattered light wavelength (EPW frequency) spacing matches well with LDI cascade theory[7,8]. In Fig. 9c, the scattered light spectrum is broadened towards shorter wavelengths (lower EPW frequencies), and the broadening is quantitatively consistent with the nonlinear frequency shift due to electron trapping[7]. For trapping, the frequency

shift occurs on sub-psec time scales as the driven EPW grows and decays. Since $\partial\lambda/\partial t >> \Delta\lambda/\Delta t$ in this case, broadening is observed in the trapping regime rather than a chirped nonlinear frequency shift[7]. An intermediate regime is observed in Fig. 9b. Overplotted on Fig. 9a is a bar indicating the spectral width of Thomson scattered light from EPW from a similar experiment using a RPP laser to drive SRS [see Fig. 2 of Ref. 10]. As can be easily seen, EPW are driven over a broad range of frequencies due to plasma inhomogeneity in the RPP experiment, and one cannot readily discern sufficient details regarding nonlinear behavior from those experiments[3].

Finally, we show angle-resolved spectra [so-called (ω, k) diagnostic[9]] from EPW in the LDI cascade regime in Fig. 10. The primary EPW from SRS is labeled as k_1, and two co-propagating waves (k_3, k_5) generated by at least 4 LDI cascade steps are clearly observed. The angular range of the optics prohibited detection of further possible LDI steps. Using the wave matching conditions, the scattered light wavelength and scattering angle can be directly related to (ω, k). The Δk and $\Delta\omega$ in this experiment is in excellent agreement with LDI theory[7, 8]. This data can be qualitatively compared to Fig. 2 of Ref. 11, where (ω, k) EPW spectra from a RPP experiment are shown. In that experiment, LDI cascade can only be inferred by general trends in the (ω, k) spectra[11], and not fully resolved as discrete steps as in the single hot spot experiment.

V. Summary and Conclusions

Small plasma sizes in laser-produced plasmas make diagnosis a challenge, especially in the presence of plasma inhomogeneity. To overcome these limitations, two techniques were developed for Thomson scattering in laser-plasmas. To measure wave

damping in inhomogeneous plasmas, imaging Thomson scattering is used. The unavoidable broadening due to plasma inhomogeneity is accounted for by measuring spatially-resolved profiles of scattering from IAW and EPW. The broadening is modeled, and allows a determination of wave damping. For nonlinear wave effects, inhomogeneity broadening is avoided by using a diffraction-limited laser beam to drive nonlinear waves. The comparatively small interaction volume means that the driven waves occur in extremely homogeneous conditions, allowing detection of subtle nonlinear behavior. The data quality is vastly improved compared to Thomson scatter data from RPP experiments.

The authors gratefully acknowledge useful discussions with J.F. Benage, R.P. Johnson, and F.J. Wysocki, and the dedicated efforts of the Trident laser crew. This work was performed under the auspices of the NNSA/DOE by the Los Alamos National Laboratory under contract number W-7405-ENG-36.

References

1. W.L. Kruer, *The Physics of Laser Plasma Interactions* (Addison-Wesley, Reading MA, 1988).
2. J. Sheffield, *Plasma Scattering of Electromagnetic Radiation* (Academic, New York, 1975).
3. D.S. Montgomery, *Phys. Rev. Lett.* **86**, 3686 (2001).
4. T.E. Tierney, D.S. Montgomery, J.F. Benage, F.J. Wysocki, M.S. Murillo, *J. Phys. A* **36**, 5981 (2003); T.E. Tierney, Ph.D. thesis, Univ. of California Irvine, 2002.
5. N.K. Moncur, R.P. Johnson, R.G. Watt, R.B. Gibson, *Appl. Opt.* **34**, 4274 (1995).
6. D.S. Montgomery, R.P. Johnson, J.A. Cobble, J.C. Fernandez, E.L. Lindman, H.A. Rose, K.G. Estabrook, *Laser Part. Beams* **17**, 349 (1999).
7. J.L. Kline, D.S. Montgomery, B. Bezzerides, J.A. Cobble, D.F. DuBois, R.P. Johnson, H.A. Rose, H.X. Vu, submitted to Phys. Rev. Lett. (2003).
8. D.S. Montgomery, J.A. Cobble, J.C. Fernandez, R.J. Focia, R.P. Johnson, N. Renard-LeGalloudec, H.A. Rose, D.A. Russell, *Phys. Plasmas* **9**, 2311 (2002).
9. H.A. Baldis, C.J. Walsh, *Appl. Phys. B* **28**, 293 (1982).
10. S. Depierreux, J. Fuchs, C. Labaune, A. Michard, H.A. Baldis, D. Pesme, S. Huller, G. Laval, *Phys. Rev. Lett.* **84**, 2869 (2000).
11. S. Depierreux, C. Labaune, J. Fuchs, D. Pesme, V.T. Tikhonchuk, H.A. Baldis, *Phys. Rev. Lett.* **89**, 045001 (2002).

Figure Captions

1. Schematic diagram of collective Thomson scatter
2. Setup for collisional damping experiment. The target, plasma, beam, and diagnostic geometry is shown from (a) the diagnostic view, and (b) from the heater beam view.
3. Spatially-resolved Thomson scatter IAW spectrum from an Al plasma in the ion-collisional regime.
4. Diagram of 2-D grid used to model broadening due to plasma inhomogeneity. Plasma density, temperature and flow profiles are input at each grid point, the Thomson scattering form factor is computed, and the scattered light contribution is summed within the probe volume (shaded area) for each spatial resolution point in the imaging direction.
5. Synthesized IAW spectrum for the data shown in Fig. 3.
6. Plot of spectral broadening dw/wiaw versus radial position. Experimental data from Fig. 3 shown as points, and theoretical results for a collisional form factor (solid curve) and collisionless form factor (dashed curve) are given.
7. Setup for nonlinear wave experiment using a diffraction-limited laser beam to drive instabilities. The driven waves are detected using collective Thomson scattering from a 351-nm probe.
8. Diagram showing detection of driven waves in the single hot spot experiment. The probe volume is much larger than the interaction volume in this experiment.
9. Streaked Thomson spectra from driven EPW for an experiment at (a) n_e/n_{cr} = 0.049, (b) $n_e/n_{cr} = 0.044$, and (c) $n_e/n_{cr} = 0.034$. Fig. 9a shows multiple EPW,

indicating the LDI regime, and Fig. 9c shows a frequency-broadened spectrum indicative of electron trapping. A bar is drawn in Fig. 9a showing the typical spectral width of EPW from the RPP experiment in Ref. 10, where the experimental conditions are fairly similar to the present experiment. The spectral width from an individual EPW in Fig. 9a is resolution limited at ~ 1 Å.

10. Angle-resolved spectrum [so-called (ω, k) spectrum] from a single hot spot interaction experiment in the LDI cascade regime. The scattered light wavelength and the scattering angle can be directly related to (ω, k). The SRS daughter EPW (k_1), and two co-propagating LDI steps (k_3, k_5) are indicated, demonstrating the observation of at least four discrete LDI steps driven by the SRS EPW.

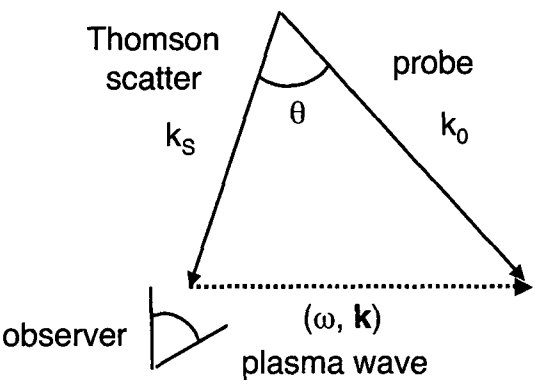

Fig. 1
D.S. Montgomery et al.
submitted to Rev. Sci. Instrum.
"Detailed Characterization of Plasma Wave
Behavior Using Collective Thomson Scattering"

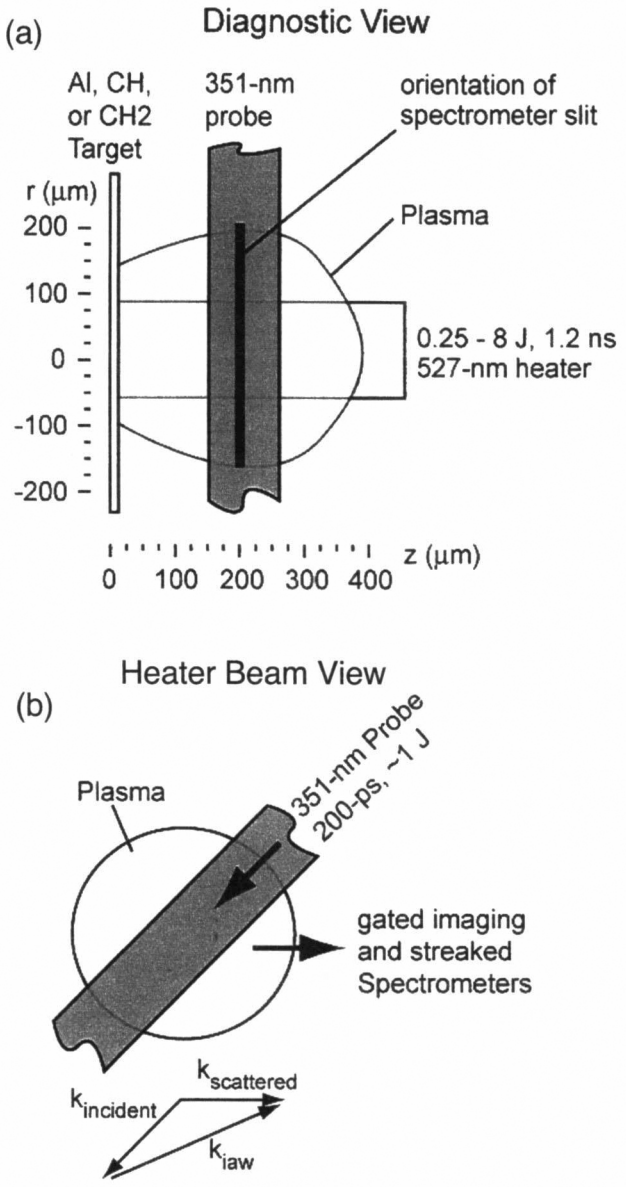

Fig. 2a - 2b
D.S. Montgomery et al.
submitted to Rev. Sci. Instrum.
"Detailed Characterization of Plasma Wave
Behavior Using Collective Thomson Scattering"

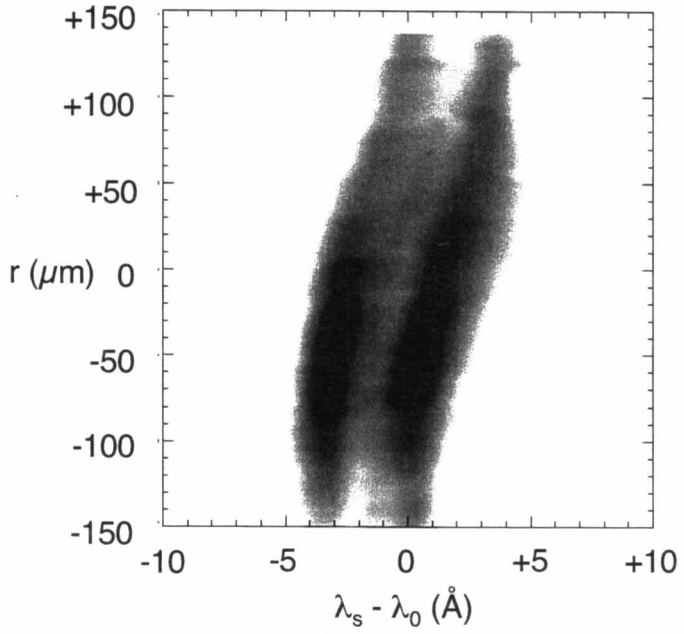

Fig. 3
D.S. Montgomery et al.
submitted to Rev. Sci. Instrum.
"Detailed Characterization of Plasma Wave
Behavior Using Collective Thomson Scattering"

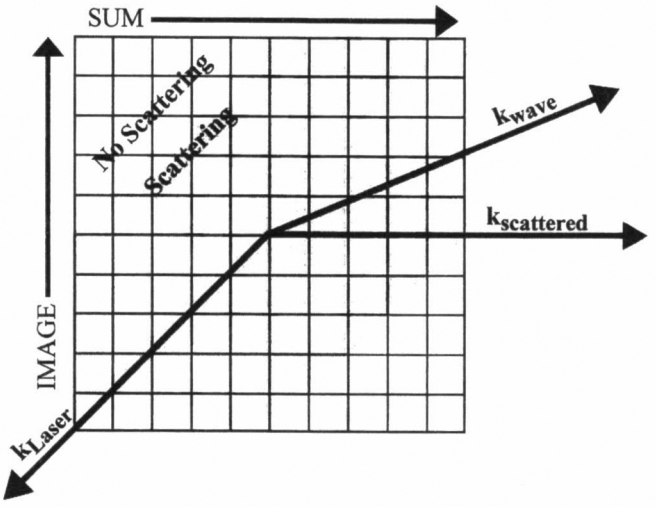

Fig. 4
D.S. Montgomery et al.
submitted to Rev. Sci. Instrum.
"Detailed Characterization of Plasma Wave
Behavior Using Collective Thomson Scattering"

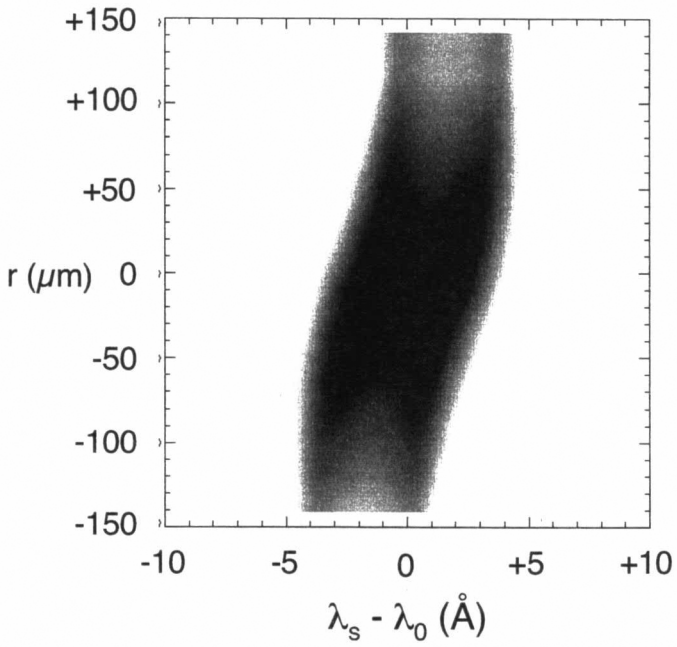

Fig. 5
D.S. Montgomery et al.
submitted to Rev. Sci. Instrum.
"Detailed Characterization of Plasma Wave
Behavior Using Collective Thomson Scattering"

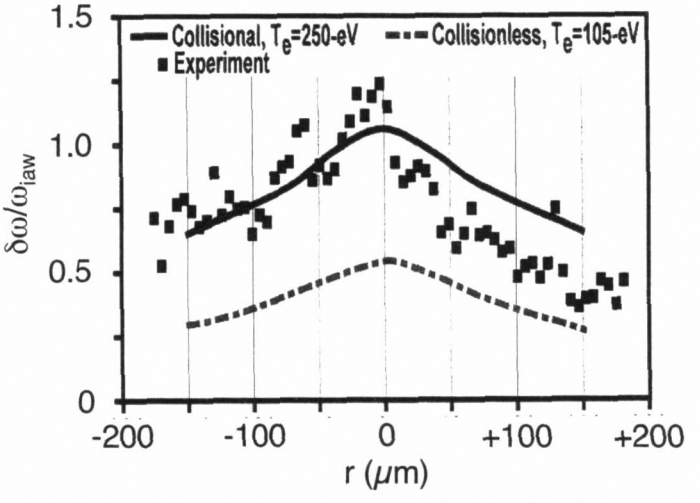

Fig. 6
D.S. Montgomery et al.
submitted to Rev. Sci. Instrum.
"Detailed Characterization of Plasma Wave
Behavior Using Collective Thomson Scattering"v

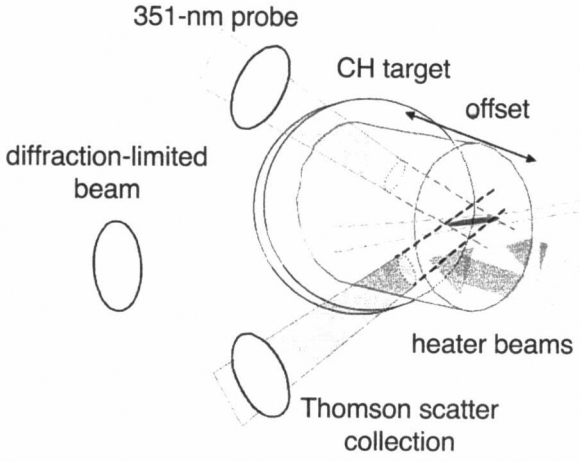

Fig. 7
D.S. Montgomery et al.
submitted to Rev. Sci. Instrum.
"Detailed Characterization of Plasma Wave
Behavior Using Collective Thomson Scattering"

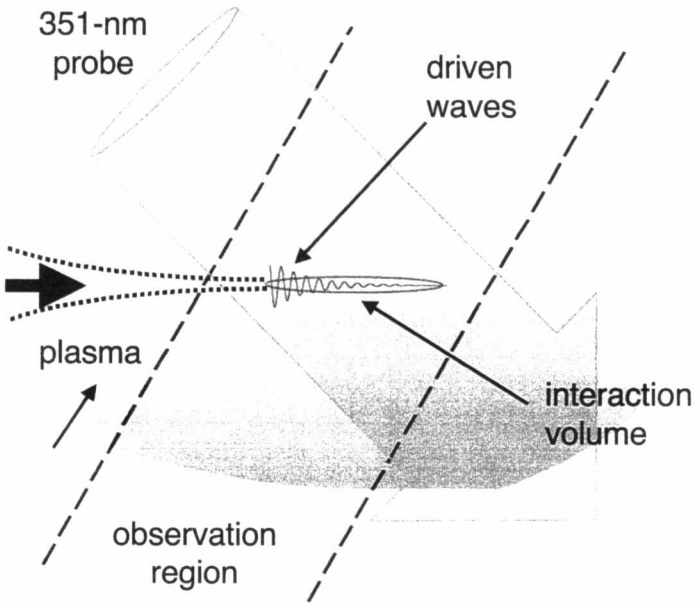

Fig. 8
D.S. Montgomery et al.
submitted to Rev. Sci. Instrum.
"Detailed Characterization of Plasma Wave
Behavior Using Collective Thomson Scattering"

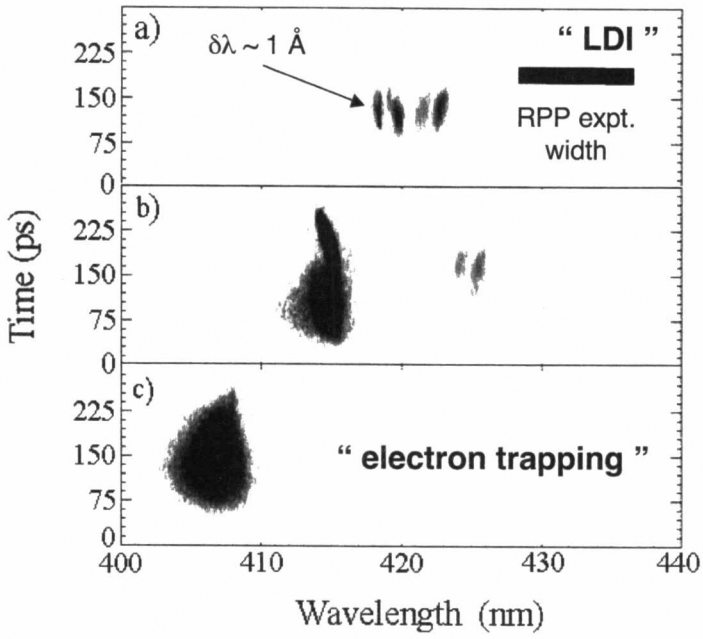

Fig. 9a - 9c
D.S. Montgomery et al.
submitted to Rev. Sci. Instrum.
"Detailed Characterization of Plasma Wave Behavior Using Collective Thomson Scattering"

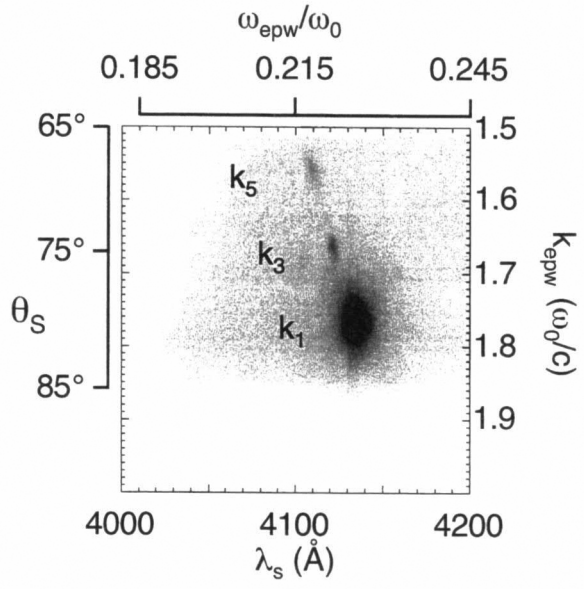

Fig. 10
D.S. Montgomery et al.
submitted to Rev. Sci. Instrum.
"Detailed Characterization of Plasma Wave
Behavior Using Collective Thomson Scattering"